

Thermodynamic Studies on the Interaction of Dioxopromethazine to β -Cyclodextrin and Bovine Serum Albumin

Hua-Xin Zhang · Xing Huang · Min Zhang

Received: 2 August 2007 / Accepted: 7 February 2008 / Published online: 23 February 2008
© Springer Science + Business Media, LLC 2008

Abstract The interaction of dioxopromethazine (DOPM) with β -cyclodextrin (β -CD) and bovine serum albumin (BSA) were investigated by fluorescence quenching method. It was shown that DOPM has quite a strong ability to quench the fluorescence launching from BSA by reacting with it and forming a certain kind of new compound. The quenching and the energy transfer mechanisms were discussed, respectively. The binding constants and thermodynamic parameters at four different temperatures, the binding locality, and the binding power were obtained. The conformation of BSA was discussed by synchronous and three-dimensional fluorescence techniques. The inclusion reaction between β -CD and DOPM was explored by both Lineweaver–Burk equation and Benesi–Hildebrand equation. The inclusion constants and the thermodynamic parameters at 297 and 307 K were figured out, respectively. The mechanism of inclusion reaction was speculated and the slow release characteristics of β -CD to DOPM was attempted to explain at molecule level.

Keywords Dioxopromethazine · β -cyclodextrin · Bovine serum albumin · Interaction · Thermodynamics · Slow release

Introduction

Dioxopromethazine (DOPM; formula: $C_{17}H_{20}N_2O_2S$; molecule weight 316.42), is a new medicine that mainly acts on respiratory system. Its effect of preventing cough is about six to 11 times as well as codeine. Besides, it also has the function of dispelling phlegm, alleviating dyspnea, relieving the spasm of smooth muscle, antihistamine, anti-inflammation and local anesthesia. It has been widely applied in acute, chronic bronchitis, allergic asthma, nettle rash and pruritus. Serum albumins are the most abundant proteins in plasma (50–60% of total amount of plasma proteins) and the main transport proteins [1, 2]. They bind metabolites, endogenous toxins, hormones etc. Interaction between serum albumins and ligands can provide important information about ligands' storage, transportation, evacuation etc. Thereupon, researches on these have attracted more and more attention of the biologist, chemist, pharmacist and therapist [2–7].

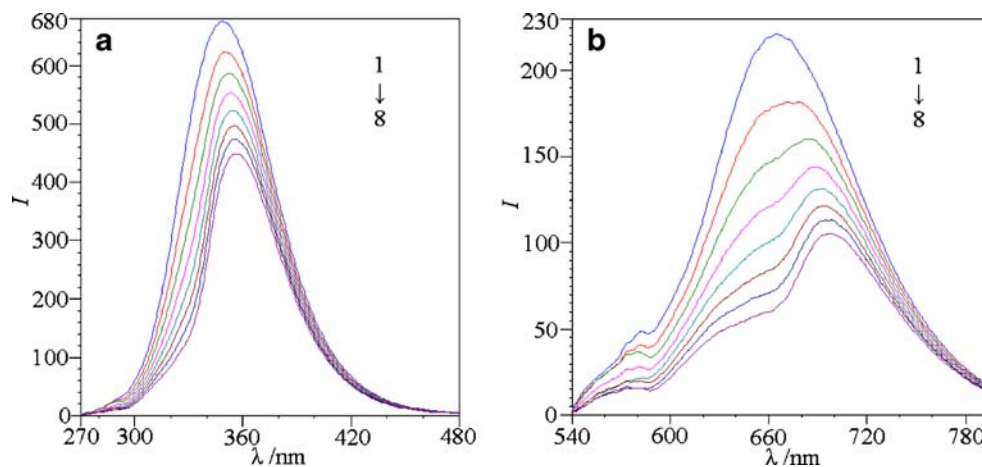
β -cyclodextrin (β -CD) is composed of seven units of D (+)-glucopyranose units joined by α -1, 4-glycosidic bonds arranged in a truncated cone-shaped structure [8]. As one of the water-soluble cyclic oligosaccharides, it can form inclusion complexes with a large variety of organic and inorganic compounds, which may improve the solubility, stability and bioavailability of guest molecules. As a result, β -CD has been widely applied in food research, organic synthesis, environment protection and especially in the area of pharmacological science [9–13].

The aim of the present work was (1) to study interaction between DOPM and bovine serum albumin (BSA); (2) to study the interaction between DOPM and β -CD; (3) to compare the thermodynamic characteristics of the former reaction with that of the latter, and to get some information on the slow release capability of β -CD to DOPM. In order to attain these objectives, fluorescence spectroscopy (including

H.-X. Zhang (✉) · M. Zhang
College of Chemical Engineering,
Jingchu University of Technology,
Jingmen, Hubei 448000, People's Republic of China
e-mail: H.X.ZHANG@yeah.net

X. Huang
College of Chemistry, Central China Normal University,
Wuhan, Hubei 430027, People's Republic of China

Fig. 1 The fluorescence spectra of BSA around 350 nm (a) and 680 nm (b) in and in no presence of DOPM ($T=297$ K). $C_{\text{BSA}}=1.000 \times 10^{-5}$ mol L $^{-1}$; $C_{\text{DOPM}}/(10^{-5}$ mol L $^{-1}$), 1–8 0, 0.6321, 1.264, 1.896, 2.528, 3.160, 3.792, 4.424



emission spectrum, three-dimensional fluorescence spectrum and synchronous fluorescence spectrum) and ultraviolet (UV)-visible absorption spectroscopy were employed when we carried out detailed investigation of DOPM–BSA association. And the inclusion reaction between β -CD and DOPM was studied by both Lineweaver–Burk equation and Benesi–Hildebrand equation.

Experimental

Materials

BSA and β -CD were both purchased from Sigma (USA). DOPM was obtained from National Institution for the Control of Pharmaceutic and Biological Products (China). Tris, HCl, NaCl were purchased from Shanghai Chemical Reagent Company (China). DOPM had a purity of no less than 99.5% and all other chemicals were of analytical grade. Stock solutions of BSA (5×10^{-5} mol L $^{-1}$), β -CD (0.0150 mol L $^{-1}$), DOPM (40 mg L $^{-1}$), NaCl (0.5 mol L $^{-1}$) and Tris–HCl buffer (0.05 mol L $^{-1}$ Tris, 0.15 mol L $^{-1}$ HCl) of pH 7.40 ± 0.01 were prepared by directly dissolving the

original reagents in water. Water used to prepare solutions was double-distilled.

Apparatus

All fluorescence measurements were carried out on an LS-55 recording spectrophotometer (Perkin-Elmer Corporate, USA). All ultraviolet-visible spectra were recorded in a UV-1100 spectrophotometer (Beijing, China). The weight measurements were performed with an AY-120 electronic analytic weighing scale (Shimadzu, Japan). All pH measurements were made with a PHS-3 digital pH-meter (± 0.01 , Shanghai, China). The specified temperatures were controlled by air conditioners and an SYS-15 digital aqueous thermostat (± 0.01 °C, Nanjing, China).

Procedure and measurement

The buffer, NaCl, DOPM, β -CD and BSA solutions were added with different ratios into several 10 mL colorimetric tubes, then diluted to 10 mL and stirred well. The solutions were let to stand for 5 min at room temperature, and then react for 30 min at specified temperatures.

Fig. 2 Stern–Volmer curves (a) and Lineweaver–Burk (b) curves of BSA with certain amount of DOPM

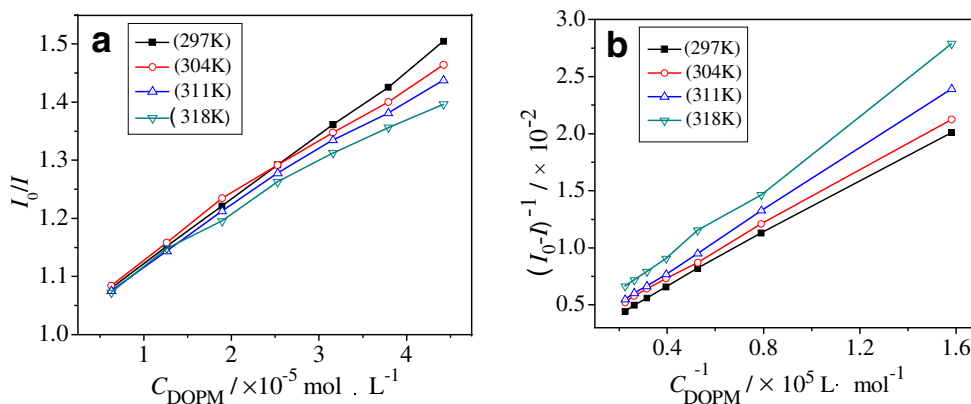


Table 1 Regression equations and correlation coefficients

Curves	T/K	Regression equations	R
A	297	$I_0/I=1.010+1.109 \times 10^4 C_{\text{DOPM}}$	0.9998
	304	$I_0/I=1.034+9.811 \times 10^3 C_{\text{DOPM}}$	0.9977
	311	$I_0/I=1.025+9.526 \times 10^3 C_{\text{DOPM}}$	0.9976
	318	$I_0/I=1.034+8.514 \times 10^3 C_{\text{DOPM}}$	0.9955
B	297	$(I_0-I)^{-1}=0.001977+1.152 \times 10^{-7} C_{\text{DOPM}}^{-1}$	0.9997
	304	$(I_0-I)^{-1}=0.002615+1.178 \times 10^{-7} C_{\text{DOPM}}^{-1}$	0.9998
	311	$(I_0-I)^{-1}=0.002354+1.364 \times 10^{-7} C_{\text{DOPM}}^{-1}$	0.9999
	318	$(I_0-I)^{-1}=0.002975+1.560 \times 10^{-7} C_{\text{DOPM}}^{-1}$	0.9990

In case of the fluorescence spectra of BSA with and without DOPM the excitation wavelength was set at 285 nm and the emission wavelength was set between 200 and 800 nm. In case of fluorescence synchronous scan spectra the wavelength shift $\Delta\lambda$ was equal to 15 and 60 nm, respectively. In case of the fluorescence spectra of DOPM with and without β -CD the excitation wavelength was set at 227 nm and the emission wavelength was set between 300 and 430 nm. The three-dimensional fluorescence spectrum was performed under the following conditions: the initial excitation wavelength at 200 nm, the emission wavelength between 200 and 800 nm, scanning number 30 and increment 5 nm with other parameters just the same to that of the fluorescence spectra of BSA. In case of absorption spectra scan the slit width was set at 1 nm and the wavelength was set between 200 and 300 nm. The excitation and emission slit widths for all fluorescence spectra were 15 and 2.5 nm and the scanning speed was set at 1,200 nm/min. Samples were contained in 1 cm path length quartz cuvettes.

Results and discussion

The fluorescence quenching spectra

Fluorescence quenching refers to any process which decreases the fluorescence intensity of a phosphor. A variety of molecular interactions can result in fluorescence quenching, including excited-state reactions, molecular rearrangements, energy transfer, ground-state complex formation, and collisional quenching [14]. The different mechanisms of fluorescence quenching are usually classified as either dynamic quenching or static quenching. Dynamic quenching and static quenching are caused by diffusion and ground-state complex formation, respectively. And they have different dependence on temperature: it is known that higher temper-

Table 2 Binding constants

T/K	$K_{\text{SV}}/\text{L mol}^{-1}$	$K_q/\text{L mol}^{-1} \text{ s}^{-1}$	$K_{\text{LB}}/\text{L mol}^{-1}$
297	1.098×10^4	1.098×10^{12}	1.716×10^4
304	9.488×10^3	9.488×10^{11}	2.220×10^4
311	9.294×10^3	9.294×10^{11}	1.726×10^4
318	7.886×10^3	7.886×10^{11}	1.907×10^4

atures result in larger diffusion coefficients, the dynamic quenching constants are expected to increase with increasing temperature. In contrast, increased temperature is likely to result in decreased stability of complexes, and thus lower values of the static quenching constants. Dynamic and static quenching can be distinguished by the absorption spectra before and after two samples interact, as well [15, 16].

In this experiment, BSA was phosphor [17] while DOPM acted as the quencher. The fluorescence spectra of BSA and its fluorescence quenching ones by DOPM, were obtained according to procedures mentioned and were shown in Fig. 1.

The fluorescence quenching mechanism

It is apparent, from Fig. 1 that the fluorescence intensity of BSA was decreased regularly with the increase of DOPM concentration, which indicates that there was a certain kind of interaction between DOPM and BSA, and the energy transfer occurred.

In order to confirm the quenching mechanism, we analyzed the fluorescence data at different temperatures with the well-known Stern–Volmer equation and Lineweaver–Burk equation, which were commonly used in describing dynamic quenching and static quenching, respectively. Supposing C_B, C_0, I_0, I are the concentration of free fluorescence object, the concentration of all fluorescence object, the fluorescence intensities in the absence and in the presence of quencher, respectively, the equation $C_B/C_0=I/I_0$ will be reasonable when the formation does not give out fluorescence in a selected wavelength range. Then the Stern–Volmer equation is [15, 16, 18]:

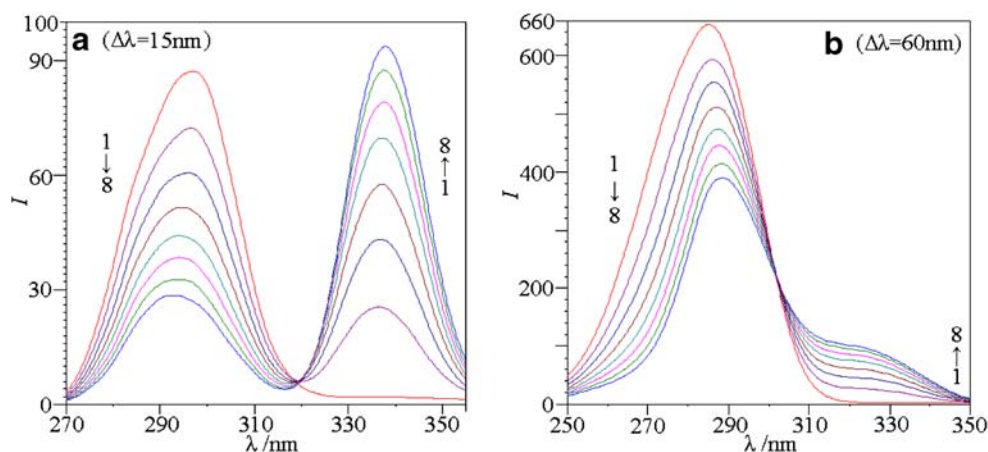
$$I_0/I = 1 + K_{\text{SV}}[Q] = 1 + K_q \tau_0 [Q] \tag{1}$$

where K_{SV} is the Stern–Volmer quenching constant with the unit of liter per mole, $[Q]$ the concentration of the quencher,

Table 3 Thermodynamic parameters derived from K_{LB}

T/K	$\Delta H^\theta/\text{kJmol}^{-1}$	$\Delta S^\theta/\text{JK}^{-1}$	$\Delta G^\theta/\text{kJmol}^{-1}$
297	3.946	94.36	-24.08
304		96.17	-25.29
311		93.81	-25.23
318		95.56	-26.06

Fig. 3 The effect of DOPM on the synchronous fluorescence spectra of BSA when $\Delta\lambda$ were set at 15 nm (a) and 60 nm (b). $C_{\text{BSA}}=1.000\times 10^{-5}$ mol L $^{-1}$; $C_{\text{DOPM}}/(10^{-5}$ mol L $^{-1}$), 1–8 0, 0.6321, 1.264, 1.896, 2.528, 3.160, 3.792, 4.424



K_q the quenching rate constant of the biological macromolecule and $K_q=K_{\text{SV}}/\tau_0$, τ_0 the average lifetime of the molecule without any quencher and the fluorescence lifetime of the biopolymer is 10^{-8} s.

Lineweaver–Burk equation is [15, 16]:

$$(I_0 - I)^{-1} = (I_0)^{-1} + K_{\text{LB}}^{-1} I_0^{-1} [Q]^{-1} \quad (2)$$

where K_{LB} is the static quenching constant with the unit of liter per mole, which describes the binding efficiency of micro-molecules to biological macromolecules at ground state.

Experiments have been done on the fluorescence quenching spectra at four different temperatures and the data have been disposed of according to Stern–Volmer's equation and Lineweaver–Burk equation respectively. These two equation curves are shown in Fig. 2 and their regression equations and correlation coefficients are in Table 1.

Reference has pointed out the maximum scatter collision quenching constant of various quenchers with biopolymer

is 2.0×10^{10} L mol $^{-1}$ s $^{-1}$ [15, 16], and it is obvious that the rate constants K_q shown in Table 2 are greater than 2.0×10^{10} L mol $^{-1}$ s $^{-1}$. From Fig. 2 and Table 1, it can be seen that the curves of Lineweaver–Burk equation have better linear relations. When attention was paid to the value of K_{SV} in Table 2, it could be found that its value became smaller and smaller when the temperature gradually rose. It is exactly the opposite to the definition of dynamic quenching, which can indicate that the quenching was not initiated by collision. Meanwhile, the absorption spectra of BSA–DOPM system are clearly different from those of BSA or DOPM alone, which is obvious evidence that they have formed at least one protein–drug complex with certain new structure. Consequently a conclusion may be safely drawn that the quenching of DOPM to BSA belongs to static quenching with complex formation. So the static binding constants were used when the thermodynamic parameters were calculated.

When the temperature change is not very enormous, the enthalpy change ΔH^θ of a system can be regarded as a constant. Under this premise, the thermodynamic parameters

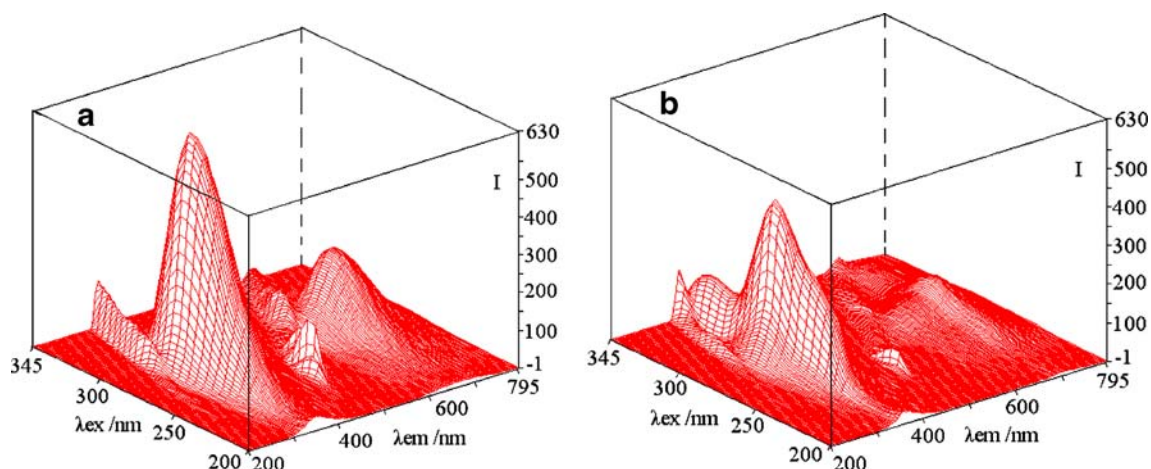


Fig. 4 Three-dimensional fluorescence spectra of BSA (a) and DOPM–BSA complex (b). $C_{\text{BSA}}/(10^{-5}$ mol L $^{-1}$), a 1.000, b 1.000; $C_{\text{DOPM}}/(10^{-5}$ mol L $^{-1}$), a 0, b 4.4244

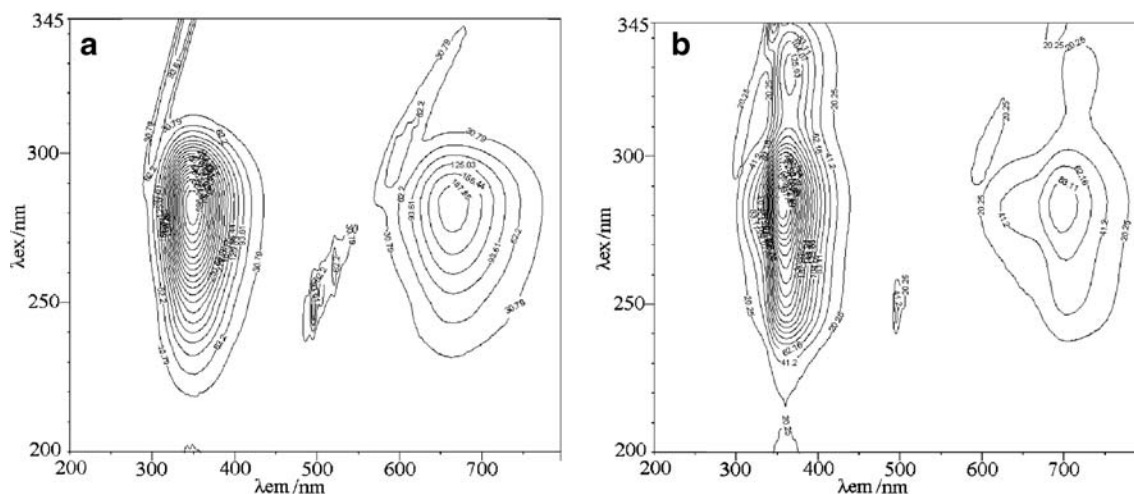


Fig. 5 Contour spectra of BSA (a) and DOPM–BSA complex (b). $C_{BSA}/(10^{-5} \text{ mol L}^{-1})$, a 1.000, b 1.000; $C_{DOPM}/(10^{-5} \text{ mol L}^{-1})$, a 0, b 4.4244

ters deriving from the static binding constants were obtained and showed in Table 3 according to the Eqs. 3–5.

$$\Delta G^\theta = -RT \ln K^\theta \tag{3}$$

$$\ln (K_2^\theta / K_1^\theta) = (\Delta H^\theta / R) \cdot (1/T_1 - 1/T_2) \tag{4}$$

$$\Delta G^\theta = \Delta H^\theta - T \cdot \Delta S^\theta \tag{5}$$

Fluorescence energy transfer mechanism

Fluorescence energy transfer can be divided into radiation energy transfer and non-radiation energy transfer. The fluorescence spectrum will usually be misshapen when energy transfer occurs [15]. Figure 1 shows that the fluorescence spectra of BSA didn't deform, which indicates the energy transfer between BSA and DOPM is not likely to be radiation energy transfer. Non-radiation energy transfer can happen not only between molecules but also within single molecule. If new complex has formed between donor and acceptor, it belongs to the latter and otherwise the former [14, 16]. Base on discussion above,

we draw a conclusion that the quenching between BSA and DOPM belongs to non-radiation energy transfer happening within single molecule.

The effect of DOPM on BSA conformation

Synchronous fluorescence spectroscopy is a common method for evaluating the conformational changes of protein. The synchronous fluorescence spectra of BSA and BSA–DOPM systems were shown in Fig. 3.

Spectroscopy is an ideal tool to observe conformational changes in proteins as it allows non-intrusive measurements of substances in low concentration under physiological conditions. It is advantageous to use intrinsic fluorophores for these investigations in order to avoid complicated labeling with an extrinsic dye. In synchronous spectra, the sensitivity associated with fluorescence is maintained while offering several advantages: spectral simplification, spectral bandwidth reduction and avoiding different perturbing effects. It has been reported that the shift in wavelength of emission maximum λ_{max} corresponds to the changes of polarity around the chromophore molecule [15, 18]. When the wavelength shift ($\Delta\lambda$) between excitation and emission wavelength were stabilized at 15 nm, the synchronous fluorescence gives the characteristic information of tyrosine

Table 4 Three-dimensional fluorescence spectral characteristics of BSA and BSA–DOPM system

Peaks	BSA			BSA–DOPM		
	Peak position ($\lambda_{ex}/\lambda_{em}$)/ (nm/nm)	$\Delta\lambda$ / (nm)	Intensity <i>I</i>	Peak position ($\lambda_{ex}/\lambda_{em}$)/ (nm/nm)	$\Delta\lambda$ / (nm)	Intensity <i>I</i>
Rayleigh scattering peaks	270/270→345/345	0	8.067→119.3	270/270→345/345	0	1.944→125.5
Fluorescence peak	285/346.5	61.5	627.6	285/356.5	71.5	418.1
Second-order scattering peaks	235/470→345/690	λ_{ex}	2.869→27.31	235/470→345/690	λ_{ex}	1.149→30.66
Second-order fluorescence peak	285/663.5	378.5	206.2	285/694	409	97.84

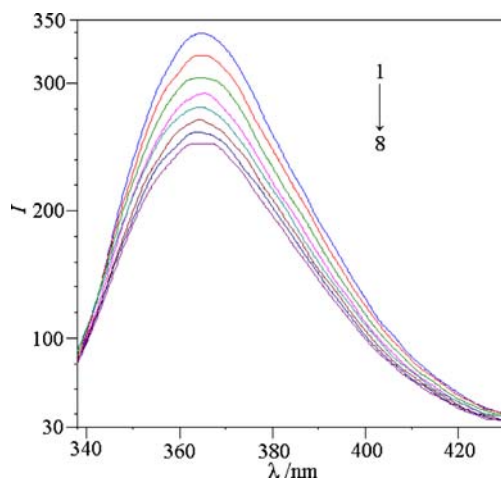


Fig. 6 Fluorescence spectra of DOPM- β -CD systems. $C_{\text{DOPM}} = 1.011 \times 10^{-5} \text{ mol L}^{-1}$; $C_{\beta\text{-CD}} / (10^{-3} \text{ mol L}^{-1})$, 1 \rightarrow 8 2.250, 2.625, 3.000, 3.375, 3.750, 4.125, 4.500, 4.875

residues. And when $\Delta\lambda$ were set at 60 nm, the spectrum characteristic of tryptophan (Trp) residues in protein was manifested. The synchronous fluorescence spectra at these two different wavelength intervals were shown in Fig. 4.

An obvious blue shift in Fig. 4a can be observed while an obvious red shift in Fig. 4b, which indicates the polarity around tyrosine residue decreased but that of tryptophan residue increased. That is to say, tryptophan residues were placed in a less hydrophobic environment and more exposed to the solvent [16]. As known to all, BSA molecule contains two of the tryptophan residues, Trp-134 and Trp-212. But we suppose that DOPM might mainly or even only bond to Trp-212 and transfer it from a position inside of a hydrophobic part of the protein molecule to an exterior. Because Trp-134 and Trp-212 are in different structure field of BSA and Trp-212 is more likely to be captured when DOPM inserts.

Besides, the three-dimensional fluorescence spectra and contour ones were shown in Figs. 4 and 5.

As known to all, normal fluorescence peaks are usually located in the lower right of the Rayleigh scattering regions. Two typical fluorescence peaks could be easily found in

three-dimensional fluorescence spectra. It was obvious that both fluorescence peaks of BSA have been quenched by DOPM, but to different extent (in presence of DOPM, the intensity ratio of fluorescence peak to second-order one is 1.501:1 while 2.108:1 in absence of it) as shown in Table 4, which indicates that DOPM has complexed with BSA to change its conformation.

Binding force

Generally speaking, the force between organic micro-molecule and biological macromolecule includes hydrophobic interaction, hydrogen bond, van der Waals force and electrostatic force. Ross etc. summed up the thermodynamic laws for estimating the type of the binding force between organic micro-molecule and biological macromolecule. That is, hydrophobic force may increase ΔH and ΔS of a system, while hydrogen bond and van der Waals power may decrease them, and electrostatic force usually makes $\Delta H \approx 0$ and $\Delta S > 0$ [19]. Based on this rule, the binding power between DOPM and BSA can be regarded as hydrophobic interaction.

Inclusion reaction of β -CD to DOPM

It is shown that β -CD has an enhanced effect on DOPM. An obvious blue shift (364 \rightarrow 343 nm) can be seen for fluorescence peak, which is a significant symbol for inclusion formation. What is interesting is that we found β -CD at relatively lower concentrations can quench the fluorescence of DOPM, which were shown in Fig. 6.

In order to identify quenching mechanism, the data have been disposed of according to Eqs. 1 and 2, respectively. These two equation curves are shown in Fig. 7 and their regression equations and correlation coefficients are in Table 5.

When temperature rose, K_{SV} decreased from 186.0 to 91.53 L mol^{-1} , which is exactly the opposite to the definition of dynamic quenching, and can indicate that the quenching

Fig. 7 Stern–Volmer curves (a) and Lineweaver–Burk (b) curves of BSA with certain concentration of DOPM

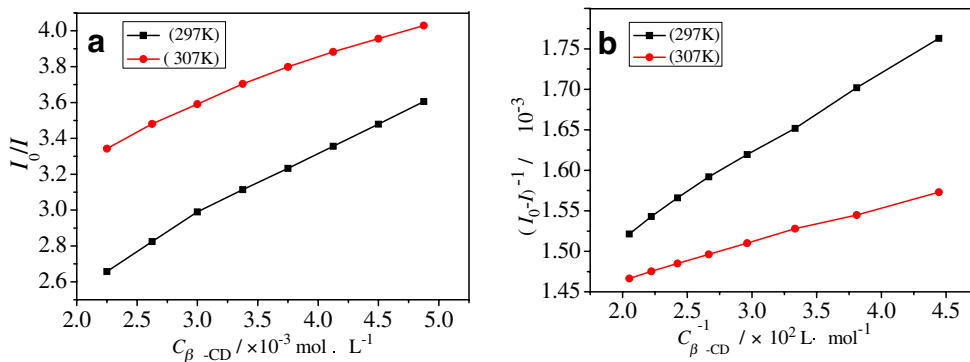


Table 5 Regression equations and correlation coefficients

Curves	T/K	Regression equations	R
A	297	$I_0/I = 1.899 + 3.533 \times 10^2 c_{\beta-CD}$	0.9978
	307	$I_0/I = 2.809 + 2.571 \times 10^2 c_{\beta-CD}$	0.9936
B	297	$(I_0 - I)^{-1} = 0.001323 + 9.943 \times 10^{-7} c_{\beta-CD}^{-1}$	0.9993
	307	$(I_0 - I)^{-1} = 0.001378 + 4.428 \times 10^{-7} c_{\beta-CD}^{-1}$	0.9991

was not initiated by collision. So we can regard it as a static quenching with inclusion formation and calculated out thermodynamic parameters shown on Table 6.

Benesi–Hildebrand method is a classical method for determining inclusion constant between drug and β -CD. The equation is [20]:

$$1/\Delta I = K_f/(\alpha \cdot c_S \cdot [\beta - CD]) + 1/(\alpha \cdot c_S) \quad (6)$$

where α is a constant, c_S , $[\beta-CD]$, K_f are total concentration of guest molecules, concentration of β -CD, inclusion constant, respectively. ΔI equals to I minus I_0 , which are the intensity of DOPM with and without β -CD. By plotting data of $1/\Delta I$ and $1/[\beta-CD]$, the K_f value can be evaluated by intercept and slope. In our experiments, c_S was fixed and $[\beta-CD]$ were replaced by C_{CD} approximately. At last, we obtained thermodynamic parameters of inclusion reaction, and they are the same with the values shown in Table 5.

Discussion on inclusion reaction mechanism

β -CD, with hydrophobic cavity of inner diameter 7 Å, can include DOPM molecule effectively. Fixed by β -CD's inner cavity, the collision frequency of DOPM molecule decreased, the absorption surface expanded. As a result, the quantum yield increased, which appears as an enhanced effect on the luminescence of DOPM. The entropy change ΔS^θ enumerated in Table 5 is 276.5 J K⁻¹ and the enthalpy change ΔH^θ is a positive value, which indicates that this inclusion interaction is spontaneous and endothermic. As a result, the inclusion constant increased when temperature rose. Considering the dimension of molecules, we think there is no possibility of accommodation of DOPM molecule completely in cavity of β -CD having a length of 7.8 Å [13, 16, 20]. So the complex formed is most likely to be the axial inclusion complex with one benzene ring of DOPM molecule outside as shown in Fig. 8.

Table 6 Binding constants and thermodynamic parameters

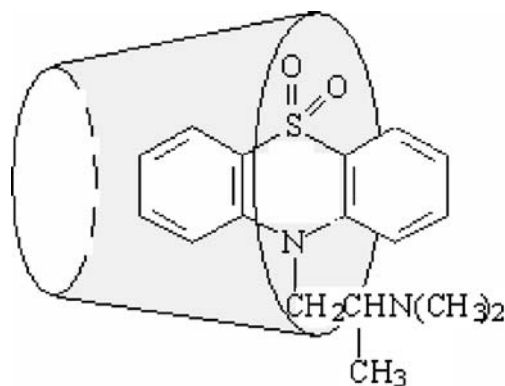
T/K	$K_{LB}(K_f)/$ L mol ⁻¹	$\Delta H^\theta/KJmol^{-1}$	$\Delta S^\theta/JK^{-1}$	$\Delta G^\theta/KJmol^{-1}$
297	1.330×10^3	64.37	276.5	-17.75
307	3.111×10^3		276.5	-20.52

Analysis on feasibility of slow release

The considerable value of inclusion constant at 307 K implicates preferable stability of β -CD–DOPM complexes, which provides a possibility for stable existence of β -CD–DOPM at temperature range of human body. Tables 3 and 6 show that the free energy ΔG^θ of DOPM–BSA formation are smaller than that of DOPM– β -CD formation, and binding constants of DOPM to BSA are much bigger than that of DOPM to β -CD when concentrations of DOPM are approximately uniform, which means DOPM could be hauled out of β -CD by BSA, and bind with protein to perform its medical effect. That is to say, β -CD can act as a good controlled releaser for DOPM.

Conclusions

This paper presents spectroscopic studies on the interaction of DOPM with β -CD and BSA using fluorescence emission spectrum, UV-visible spectrum, three-dimensional fluorescence spectrum and synchronous fluorescence spectrum. It was shown that the fluorescence of BSA has been quenched for reacting with DOPM and forming a certain kind of new compound. The quenching belonged to static fluorescence quenching, with non-radiation energy transfer happening within single molecule. The binding constant at room temperature was figured out to be 1.716×10^4 L mol⁻¹. The thermodynamic parameters agree with $\Delta G^\theta < 0$, $\Delta H^\theta > 0$, $\Delta S^\theta > 0$. The binding power between them is mainly the hydrophobic interaction. The inclusion constants between

**Fig. 8** The most probable molecular structure of β -CD–DOPM inclusion

β -CD and DOPM at 297 and 307 K were calculated to be 1,330 and 3,111 L mol⁻¹, respectively. The thermodynamic parameters comply with $\Delta G^\theta < 0$, $\Delta H^\theta > 0$, $\Delta S^\theta > 0$. β -CD has not accommodated DOPM molecule completely in its cavity but the stability of β -CD–DOPM is quite considerable at temperature range of human body. The binding constants and free energy of the two interactions indicate that β -CD not only can include DOPM effectively, but also can release it to protein gradually under close condition of concentration. So it is one of ideal slow releasers for DOPM. The next step of our work is to study of the interaction between β -CD–DOPM inclusion and human serum albumin.

References

1. Cheger SI (1975) Transport function of serum albumin. Publication of the Academy of the Socialist Republic of Romania, Bucharest, p 178
2. Scatchard G (1949) The attractions of proteins for small molecules and ions. *Ann NY Acad Sci* 51:660–672
3. Purohit G, Sakthivel Th, Florence AT (2003) The interaction of cationic dendrons with albumin and their diffusion through cellulose membranes. *Int J Pharm* 254:37–41
4. Angelakou A, Valsami G, Macheras P, Koupparis M (1999) A displacement approach for competitive drug–protein binding studies using the potentiometric-anilino-8-naphthalene-sulfonate probe technique. *Eur J Pharm Sci* 2:123–130
5. Rosso SB, Gonzalez M, Bagatolli LA, Duffard RO, Fidelio GD (1998) Evidence of a strong interaction of 2,4-dichlorophenoxy-acetic acid herbicide with bovine serum albumin. *Life Sci* 63 (26):2343–2351
6. Borga O, Borga B (1997) Serum protein binding of nonsteroidal anti-inflammatory drugs: a comparative study. *J Pharmacokinet Biopharm* 25:63–77
7. Romanini D, Avalle G, Farruggia B, Nerli B, Pico G (1998) Spectroscopy features of the binding of polyene antibiotics to bovine serum albumin. *Chem Biol Interact* 115(3):247–260
8. Szejtli J (1988) Cyclodextrin technology. Kluwer Academic, Dordrecht, pp 143–154
9. Manabe M, Ochi T, Kawamura H, Katsu-ura H, Shiomi M, Bakshi MS (2005) Volumetric study on the inclusion complex formation of α - and β -cyclodextrin with 1-alkanols at different temperatures. *Colloid Polym Sci* 283:738–746
10. Partanen R, Ahro M, Hakala M, Kallio H, Forssell P (2002) Microencapsulation of caraway extract in β -cyclodextrin and modified starches. *Eur Food Res Technol* 214:242–247
11. Cai WS, Yu YM, Shao XG (2005) Chiral recognition of aromatic compounds by β -cyclodextrin based on bimodal complexation. *J Mol Model* 11:186–193
12. Szejtli J, Sebestyén G (1979) Resorption, metabolism and toxicity studies on the peroral application of beta-cyclodextrin. *Starch* 31:385–389
13. Harada A (2001) Cyclodextrin-based molecular machines. *Acc Chem Res* 34(6):456–464
14. Lakowicz JR (1999) Principle of fluorescence spectroscopy, 2nd edn. Plenum, New York, p 13
15. Yan CN, Zhang HX, Liu Y, Mei P, Li KH, Tong JQ (2005) Fluorescence spectra of the binding reaction between paraquat and bovine serum albumin. *Acta Chimi Sin* 63:1727–1732
16. Zhang HX, Huang X, Mei P, Li KH, Yan CN (2006) Studies on the interaction of tricyclazole with β -cyclodextrin and human serum albumin by spectroscopy. *J Fluoresc* 16(3):287–294
17. Stryer L (1968) Fluorescence spectroscopy of proteins. *Science* 162(853):526–533
18. Vaughan WM, Weber G (1970) Oxygen quenching of pyrenebutyric acid fluorescence in water: a dynamic probe of the microenvironment. *Biochemistry* 9:464–473
19. Ross DP, Subramanian S (1981) Thermodynamics of protein association reactions: forces contributing to stability. *Biochemistry* 20:3096–3102
20. Muthu Vijayan Enoch IV, Swaminathan M (2004) Inclusion complexation of 2-amino-7-bromofluorene by β -Cyclodextrin: spectra characteristics and the effect of pH. *J Fluoresc* 14:751–756